

3D bioprinting of cell-laden carbopol bioinks

Original

3D bioprinting of cell-laden carbopol bioinks / Baruffaldi, D.; Pirri, C. F.; Frascella, F.. - In: BIOPRINTING. - ISSN 2405-8866. - ELETTRONICO. - 22:(2021), p. e00135. [10.1016/j.bprint.2021.e00135]

Availability:

This version is available at: 11583/2922714 since: 2021-09-09T17:37:09Z

Publisher:

Elsevier B.V.

Published

DOI:10.1016/j.bprint.2021.e00135

Terms of use:

This article is made available under terms and conditions as specified in the corresponding bibliographic description in the repository

Publisher copyright

Elsevier postprint/Author's Accepted Manuscript

© 2021. This manuscript version is made available under the CC-BY-NC-ND 4.0 license
<http://creativecommons.org/licenses/by-nc-nd/4.0/>. The final authenticated version is available online at:
<http://dx.doi.org/10.1016/j.bprint.2021.e00135>

(Article begins on next page)

Surveillance of Metropolitan Anthropic Activities by WDM 10G Optical Data Channels

Rudi Bratovich⁽¹⁾, Fransisco Martinez R.⁽¹⁾, Stefano Straullu⁽²⁾, Emanuele Virgillito⁽³⁾, Andrea Castoldi⁽¹⁾,
Andrea D'Amico⁽³⁾, Francesco Aquilino⁽²⁾, Rosanna Pastorelli⁽¹⁾, Vittorio Curri⁽³⁾

⁽¹⁾ SM-Optics, Italy, rudi.bratovich@sm-optics.com, ⁽²⁾ LINKS Foundation, Italy, ⁽³⁾ Politecnico di Torino, Italy

Abstract We propose and experimentally verify the detection via 10G channels of SOP temporal variations induced by anthropic activities. Data acquired from a metropolitan optical cable show the effective application of the proposed technique in monitoring and classifying road traffic. ©2022 The Author(s)

Introduction

Data network infrastructures are continuously expanding to support the increase in the Internet traffic demand. Wavelength Division Multiplexed (WDM) optical transmission is fast expanding as the physical layer technology from core to metro and access network segments. Thus, fiber optic cables are becoming pervasive infrastructures in most of geographical areas and specifically in highly anthropized regions.

Besides being an ultra-high capacity transmission medium, the optical fiber is an excellent sensor of mechanical stresses modifying signal phase and state of polarization (SOP), so it is extensively used in dedicated sensing equipment. Recently, the use of deployed fiber cables in production networks also for sensing purposes has been proposed, by using dedicated apparels co-existing with data traffic channels, or by directly exploiting WDM data channels.

Solutions based on dedicated equipment make use of phase sensitive optical time-domain reflectometers (OTDR)s, of distributed acoustic sensors (DAS)s or of an interferometric setup using a high coherence metrology-grade optical source.

These solutions proved excellent performance in detecting and localizing events. DAS and OTDR are effective on few tens of km, while interferometric solutions are effective also on larger reach, but requiring expensive and delicate equipments. The capability of interferometric setups in detecting and localizing earthquakes from submarine cables is shown in^[1]. In^{[2],[3]}, a DAS is used for underwater pressure wavefront detection. In^[4], an earthquake was detected using a DAS. In^{[5]-[7]}, the anthropic activity was sensed, in^{[6],[7]} road traffic was monitored and in^[5] abnormal events near/on the fiber cable were detected.

The alternative to dedicated equipment is the use of deduction of variations of SOP and/or phase from in-service optical data channels. Thanks to the channel equalizer in coherent receivers, SOP and phase variations can be retrieved from the DSP. Variations of SOP are followed by the channel equalizer, so commercial coherent transceivers (TRX)s can be used also for sensing purposes provided that DSP data are available, while for phase detection a ultra-narrow local oscillator is necessary. Using data from commercial TRXs allows event detection, while localization needs the combined used of multiple detections. In^{[8],[9]} underwater earthquakes are detected by SOP infos from commercial TRX on a trans-oceanic optical cable. The same measurement is proposed in^[10] with a purpose built coherent transceiver adding the phase detection. In^{[1],[8]} also event localization is obtained with a double pass forward propagation setup.

Despite the expansion of coherent optical technologies, 10G solutions based on polarized intensity-modulated signals are still extensively used in the access and metro network segments. Thanks to their polarized nature, SOP variations can be observed on 10G data channels by tap-

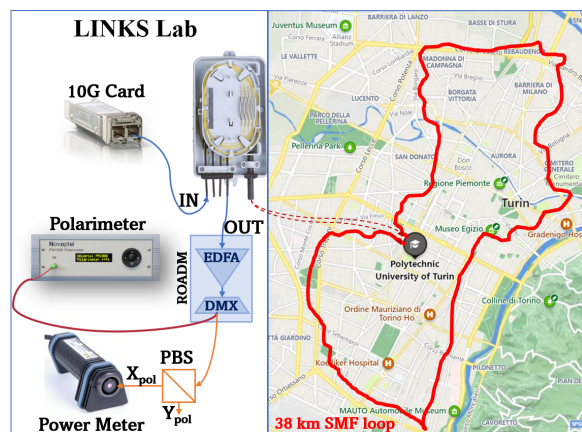


Fig. 1: Measurements Setup and map of the cable

ping out a portion of the received signal without disturbing the data transmission. SOP variations can be detected using a Polarization Beam Splitter (PBS), keeping the setup simple and low cost.

In this work, we present an experimental proof-of-concept of the proposed technique using a commercial 10G transceiver over a deployed 38 km metropolitan fiber cable. We show that using a PBS-based setup, anthropic activities can be observed on SOP variations. Results on road traffic detection and classification are displayed confirming the effectiveness of the proposed technique.

Experimental setup and measurements

The measurement setup is depicted in Fig.1. At the transmitter side, a commercial WDM card equipped with a SFP+ TRX module is used as optical source. Such signal is intensity modulated at 10 Gbps, so carrying data. The optical signal is propagated through the 38 km fiber deployed under the city of Turin, which is accessible on both ends from an optical terminal box at the LINKS laboratory.

The signal is received by a commercial ROADM with embedded EDFA and a DWDM filter, used as pre-amplifier and 10G dropping node, respectively. Two alternative receiver configurations for polarization change detection have been tested. As benchmark, we measure the SOP evolution using a commercial polarimeter (Novoptel PM-1000). The second simply monitors the power fluctuations of a single polarization state over time by means of the cascade of a PBS and an optical power meter (OPM). Both methods were set up to store up to 96 hours of measurements with a sampling rate of 95 samples per second (SpS).

In Fig.2, we show the detected SOP using the

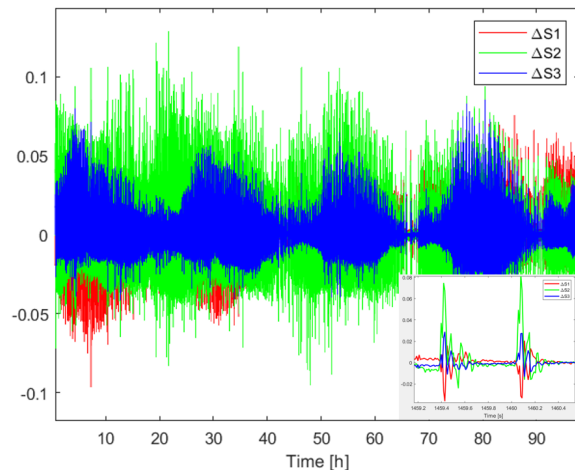


Fig. 2: Stokes parameters variation in the 96 hours measurement

polarimeter during the 96 hours measurement started at 9.30 a.m. on Friday. To focus on anthropic activities, we removed the slow SOP evolution due to daily temperature variations.

Each vertical line corresponds to a couple of peaks whose example can be seen in the figure insight. The observation clearly shows a daily variation of the peaks' amplitude and frequency with higher and more frequent peaks during the day, and smaller and less frequent peaks during the night, especially between 0.00 and 4.30 a.m.: this behavior is compatible with the road traffic daily pattern. The couples of peaks are caused by the local birefringence modulation induced by vibration/pressure produced by the passage of the front and rear car's axle across high sensitivity points, like the mini/micro trenches for fiber cable installation on the roadway. Although not visible in Fig.2, there are periodic bursts of peaks' couples, compatible with the traffic lights timing. In Fig.3 we show 11 hours results from the PBS setup: the obtained waveform is equivalent to that of Fig.2 at the same hours of the day. The Fig.3 insight shows an example of the peaks couple waveform.

Data Post-Processing and Results

Data from the 96-hours measurements have been analyzed in details focusing on the S_3 signal, which has been tested carrying the needed information. Road traffic monitoring is given by recognizing and counting signal peaks in a noisy background in the time domain. Main sources of noise are: receiver/instrumentation electronics, thermal/mechanical drift, civil structures resonance, overlapping multiple peaks, any other anthropic activities in urban environment. First, the signal is band-pass filtered to increase the signal-to-noise-

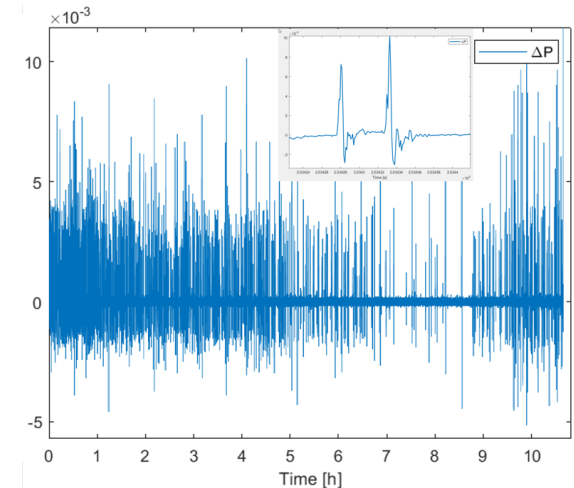


Fig. 3: 11h measurement with polarizing beam splitter and power meter

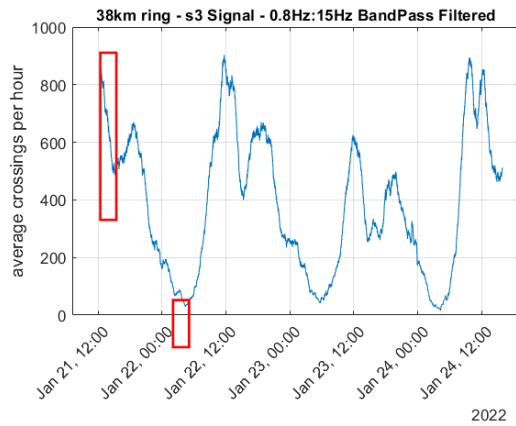


Fig. 4: Average peak count over one hour interval versus time. Rectangles show the time intervals detailed in Fig.5 and Fig.6

ratio in the time domain. The spectral analysis shows that most of the information due to road traffic is in the 1 to 15 Hz bandwidth. 0.8 Hz and 15 Hz Cutoff frequencies, 60 dB stop-band attenuation, 0.1 dB pass-band ripple were selected for the FIR filter. Then, the signal is smoothed using a Pseudo-Gaussian algorithm - and analyzed in the time domain by a peak detection algorithm optimized for narrow peaks. The peak detection algorithm is based on first derivative zero-crossings detection, with customized amplitude and slope thresholds to control peak sensitivity. The post-processing outcome is reported in Fig.4, showing the average peak counts on one hour interval vs the observation time window of 96 hours. This graph shows the average count of crossings of single wheel or wheel axle, detected by vibration-sensitive fiber sections all over the 38 km ring. The post-processing reveals evident hourly and daily seasonality in road traffic intensity. For instance, day versus night, rush hour versus lunchtime and weekdays vs. Sunday (January 23) differences are clearly readable and well compatible with the expected time pattern. Fur-

thermore, we focused on two different 3-hours intervals: one during working hours (on Friday, January 21, 12:00 to 15:00), the other at night/dawn (on Saturday, January 22, 02:00 to 05:00), represented by the two red rectangles lying over the graph in Fig.4. In these time windows, the time lag between adjacent peaks (i.e. adjacent wheel crossings) was calculated and plotted in two histograms, shown in Fig.5 (working hours) and Fig.6 (night time). The x-axis has been restricted to focus on the histogram peak at small time lags. The histograms were fitted with Log-Normal distributions (Kolmogorov-Smirnov test 3-parameters best fit)^[11] and the distribution peak time (mode) is compared for daytime (0.32s) versus nighttime (0.22s) traffic. Since the histogram peak at small time lag is now under analysis, time lag between adjacent crossings here represents the time lag between front wheelbase and rear wheelbase of one vehicle crossing a vibration-sensitive spot of the fiber ring. Therefore, it is possible to estimate the most likely vehicle speed based on the distribution peak time. Considering a typical 3 m wheelbase for commonly available cars, an estimate of 34km/h and 49km/h is made respectively, showing lower average driving speed in daytime intense road traffic than in nighttime low traffic.

Conclusion

We have proposed a suitable and low cost methodology to survey anthropic activities by detecting SOP variations by tapping out a 10G data signal. Results of the effective application of the proposed technique on an metropolitan cable are shown targeting the detection and classification of road traffic. The proposed technique is a low-cost alternative to the SOP detection from coherent TRX that can be used in metro network segment where 10G channels are still extensively used.

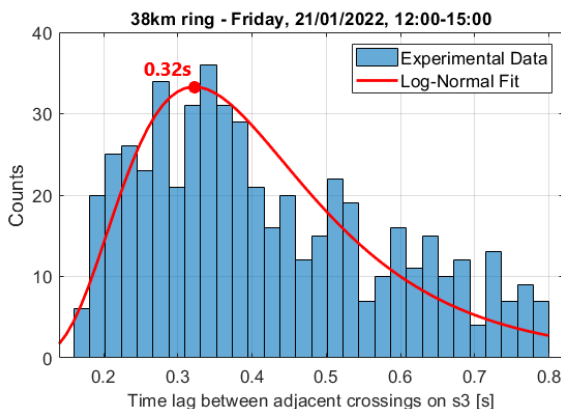


Fig. 5: Histogram of time lag between adjacent peaks, during working hours (Friday, Jan 21, noon)

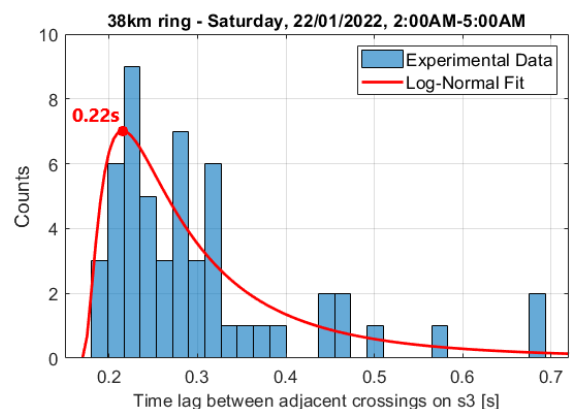


Fig. 6: Histogram of time lag between adjacent peaks at nighttime (Saturday, Jan 22, 2.00 a.m.)

References

- [1] G. Marra, C. Clivati, R. Lockett, *et al.*, “Ultrastable laser interferometry for earthquake detection with terrestrial and submarine cables”, *Science*, vol. 361, no. 6401, pp. 486–490, 2018.
- [2] H. Matsumoto, E. Araki, T. Kimura, *et al.*, “Detection of hydroacoustic signals on a fiber-optic submarine cable”, *Scientific reports*, vol. 11, no. 1, pp. 1–12, 2021.
- [3] A. Sladen, D. Rivet, J.-P. Ampuero, *et al.*, “Distributed sensing of earthquakes and ocean-solid earth interactions on seafloor telecom cables”, *Nature communications*, vol. 10, no. 1, pp. 1–8, 2019.
- [4] M. Gonzalez-Herraez, M. R. Fernandez-Ruiz, R. Magalhaes, *et al.*, “Distributed acoustic sensing for seismic monitoring”, in *Optical Fiber Communication Conference (OFC) 2021*, Optica Publishing Group, 2021, Tu1L.2.
- [5] T. Wang, M.-F. Huang, S. Han, and C. Narisetty, “Employing fiber sensing and on-premise ai solutions for cable safety protection over telecom infrastructure”, in *Optical Fiber Communication Conference (OFC) 2022*, Optica Publishing Group, 2022, Th3G.1. DOI: 10.1364/OFC.2022.Th3G.1. [Online]. Available: <http://opg.optica.org/abstract.cfm?URI=OFC-2022-Th3G.1>.
- [6] M.-F. Huang, M. Salemi, Y. Chen, *et al.*, “First field trial of distributed fiber optical sensing and high-speed communication over an operational telecom network”, *J. Lightwave Technol.*, vol. 38, no. 1, pp. 75–81, Jan. 2020.
- [7] Y.-K. Huang and E. Ip, “Simultaneous optical fiber sensing and mobile front-haul access over a passive optical network”, in *Optical Fiber Communication Conference (OFC) 2020*, Optica Publishing Group, 2020, Th1K.4.
- [8] A. Mecozzi, M. Cantono, J. C. Castellanos, V. Kamalov, R. Muller, and Z. Zhan, “Polarization sensing using submarine optical cables”, *Optica*, vol. 8, no. 6, pp. 788–795, Jun. 2021.
- [9] Z. Zhan, M. Cantono, V. Kamalov, *et al.*, “Optical polarization-based seismic and water wave sensing on transoceanic cables”, *Science*, vol. 371, no. 6532, pp. 931–936, 2021.
- [10] M. Mazur, J. C. Castellanos, R. Ryf, *et al.*, “Transoceanic phase and polarization fiber sensing using real-time coherent transceiver”, in *Optical Fiber Communication Conference (OFC) 2022*, Optica Publishing Group, 2022, M2F.2.
- [11] S. Yin, Z. Li, Y. Zhang, D. Yao, Y. Su, and L. Li, “Headway distribution modeling with regard to traffic status”, in *2009 IEEE Intelligent Vehicles Symposium*, 2009, pp. 1057–1062.